Catalysis Science & Technology

Accepted Manuscript

ROYAL SOCIETY OF CHEMISTRY

www.rsc.org/catalysis

Journal Name

ARTICLE

Selective conversion of styrene oxide to 2-phenylethanol in cascade reactions over non-noble metal catalysts

Received 00th January 20xx,
Accepted 00th January 20xx

DOI: 10.1039/x0xx00000x

www.rsc.org/

Alexandra Sasu[a,b], Brindusa Dragoi[b]*, Adrian Ungureanu[b], Sébastien Royer[c], Emil Dumitriu[b], Vasile Hulea[a]*

The catalytic hydrogenation of styrene oxide (SO) and phenylacetaldehyde (PAA) to 2-phenylethanol (2-PEA), with H2 in tri-phase system, was investigated under various reaction conditions using supported Co and Ni metal catalysts. The catalysts were produced from tri-component layered double hydroxides (i.e., hydrotalcite-like compounds (Ni)CoMgAl with 1:1:1 molar ratios), after calcination and reduction of the layered double hydroxides precursors. Among the tested solids, metallic Co-based catalyst has proven to be an efficient material for the selective hydrogenation of PAA towards 2-PEA. Taking into account the high activity and selectivity of Al-SBA-15 for SO isomerization to PAA, a two-step process was proposed as an original and highly selective route for producing 2-PEA from SO. This process involves cheap catalysts and it includes a first step of SO isomerization reaction over a mild acid strength mesoporous solid followed by hydrogenation of the resulted PAA over a redox metallic catalyst.

Introduction

Due to its distinctive odor of rose and its bacteriostatic and antifungicidal properties, 2-phenylethanol (2-PEA) is widely used in the formulation of cosmetics (perfumes, deodorants, soaps, creams, and shampoos), detergents, food additives etc.[1-4] 2-PEA is also used as starting reagent for the preparation of major chemical intermediates such as phenylacetaldehyde, phenylacetic acid and benzoic acid.[5] Conventionally, 2-PEA is synthesized through several unsustainable and dangerous processes, such as Grignard synthesis (starting from chlorobenzene and diethyl magnesium chloride) and Friedel-Crafts alkylation (from benzene and ethylene oxide, using equimolar quantity of $AlCl_3$ toward reactants).[2,5,6] In addition to safety aspects, these processes produce large amounts of undesirable wastes. 2-PEA is also obtained as a by-product in the propylene oxide production process.[2] It is recovered from a heavy residue using a strong inorganic acid, at temperatures between 150 °C and 250 °C. In order to overcome these problems, the development of efficient alternatives, using environmentally friendly agents, is highly desired. A cleaner alternative to the classical processes is the heterogeneous catalytic hydrogenation of styrene oxide (SO) to 2-PEA, using molecular hydrogen. SO is currently prepared by epoxidation of styrene with peroxybenzoic acid, but effective methods based on the styrene reaction with H_2O_2, as a green epoxidation agent, were reported.[7,8] SO hydrogenation to 2-PEA has been studied in the presence of various metallic catalysts and supports, such as Ni Raney,[9,10] Ni/saponites,[11] Ni/hectorite,[12] Ni/C, Ni/HY,[13] Ni/MgO-Al_2O_3 prepared from Ni-Mg-Al layered double hydroxides,[14] Ni/MgO,[15,16] Pd/C,[9,13,17,18] Pd/MgO, Pd/Al_2O_3, Pd/chitosan,[17,19] Pd-Cu/polyurea,[20,21] Pt/C, Pt/MgO, Pt/Al_2O_3,[22] Ru/C.[13] Although some results are promising, the most part of catalysts is not quite selective and various undesired reactions are activated including deoxygenation, over-hydrogenation and isomerization of SO, resulting in the production of ethylbenzene (EB), styrene (ST) and phenylacetaldehyde (PAA) as main by-products. For example, Mitsui et al. compared the product distribution patterns obtained for the hydrogenation of styrene oxide over different catalysts: Pd/C, PtO_2, Pt black and Raney Ni. [9] The maximum selectivity to 2-PEA was 92% over PtO_2 catalyst but the formation of EB in significant amounts (about 8%) was also observed.

In order to prevent side reactions, and to improve the selectivity to 2-PEA during SO hydrogenation with H_2 over metallic catalysts, some interesting approaches have been considered. The most effective among them seems to be the addition of a basic solution to the reaction medium.[9,13,18] Thus, complete conversion of SO, with hydrogenation selectivity towards 2-PEA above 99%, was obtained in a single step using an alkali promoted 1%Pd/C catalyst.[13] However, the basic medium can favour condensation reactions and generates some environmental problems.

Medina's group reported that the acid-base properties of the support play a major role on the selectivity during SO hydrogenation.[15,17,22] Performing the hydrogenation reaction in gas-phase, with Pd as catalyst, they found that acidic supports such as Al_2O_3 and C mainly favor side reactions. On the contrary, basic

---

[a] Institut Charles Gerhardt Montpellier, UMR 5253 CNRS/ENSCM/UM2/UM1, 8, rue de l'Ecole Normale, 34296 Montpellier cedex 5 (France).
*E-mail : vasile.hulea@enscm.fr
[b] Faculty of Chemical Engineering and Environmental Protection, "Gheorghe Asachi" Technical University of Iasi, 71 D. Mangeron Ave., 700050, Iasi, Romania.
*E-mail : bdragoi@tuiasi.ro
[c] Université de Poitiers UMR 7285 CNRS, IC2MP, 4 Rue Michel Brunet, 86022 Poitiers, France.

supports, like MgO, favor selective conversion of SO into 2-PEA. More recently, Yadav and Lawate reported that a complete conversion of SO, with 100% selectivity to 2-PEA, was obtained when the hydrogenation reaction is carried out using bimetallic Pd-Cu catalyst encapsulated in polyurea and supercritical CO_2 as a solvent.[20] In Table 1 are summarized the representative results obtained in the SO hydrogenation using various catalysts and conditions.

Table 1. Representative results in SO hydrogenation.

Catalyst	Reaction conditions	Reaction time (h)	Conversion (%)	Selectivity to 2-PEA (%)	Reference
Reaction in batch mode					
5% Pd/C	Solvent: **methanol**, T = 28 °C, pressure = 15 atm	6	96.8	98.5	10
Ni Raney			46.9	99.0	
1.6 % Ni/saponite	Solvent: **ethanol**, catalyst/SO = 1g/2mmol, room temperature, atmospheric pressure	2	25	10	11
20 % Ni/saponite		1	100	100	11
5% Ni/hectorite	Solvent: **ethanol**, catalyst/SO = 1g/2mmol, room temperature, atmospheric pressure	1	40	100	12
10% Ni/hectorite			100	100	
1% Pt/C	Solvent: **methanol**, catalyst/SO = 0.375 g/0.416 mol, T = 40 °C, P = 20.5 atm, Conc. of NaOH : 0.013 kg/m^3		70	88	13
1% Pd/C			100	99	
10% Ni/C			60	85	
2% Ru/C			82	87	
73-80 % Ni/MgO-Al_2O_3	Solvent: **ethanol**, catalyst (active phase)/SO = 1.5 g/4 mmol, room temperature, atmospheric pressure	1	100	> 90	14
2% Pd/chitosan	Solvent: **methanol**, T = 40 °C, pressure = 20 atm	1	57	90	19
1 % Pd/C	Solvent: **ethanol/water** (30:70), T = 50 °C, pressure = 2.4MPa		TOF = 0.13 x $10^{-5}h^{-1}$	51	23
1 % Ru/C			TOF = 0.08 x $10^{-5}h^{-1}$	65	
1 % Ni/C			TOF = 0.01 x $10^{-5}h^{-1}$	51	
Reaction in flow mode					
0.2% Pd/MgO	T = 125 °C, atmospheric pressure, 0.1 g catalyst, WHSV= 30000 h^{-1}, H2/SO = 20 mol/mol	-	88	90	17
2% Pd/MgO	T = 125 °C, atmospheric pressure, 0.1 g catalyst, WHSV= 10000 h^{-1}, H2/SO = 20 mol/mol	-	99.5	99.2	
2% Pd/g-Al_2O_3	T = 125 °C, atmospheric pressure, 0.1 g catalyst, WHSV= 30000 h^{-1}, H2/SO = 20 mol/mol	-	99.5	16	

2-PEA could be also produced by catalytic hydrogenation of PAA. Few results are available in literature about this process, and it is reported only the use of cationic Rh complexes[24] and Pt/TiO_2[25] as catalysts.

The aim of this work was to propose new catalysts to design an integrated process for the selective conversion of SO into 2-PEA. For this purpose, the hydrogenation of both SO and PAA with H_2, was performed over Co- and Ni-based catalysts, as cheap and widely available non-noble metals. Catalysts were obtained from layered double hydroxides (LDH) precursors. To the best of our knowledge, there is no report on the hydrogenation of SO using Co-based catalysts. An original two-step process, including the SO isomerization into PAA (over an acid catalyst: Al-SBA-15),[26] followed by the PAA hydrogenation into 2-PEA (over Co-based catalyst), was designed as efficient route for the selective production of 2-PEA from SO.

Experimental

Materials.

All chemicals required to prepare mesoporous Al-SBA-15 and LDH catalysts were used as purchased: tetraethylorthosilicate ($Si(OC_2H_5)_4$, TEOS, 98%, Aldrich), non-ionic triblock co-polymer Pluronic P123 (poly(ethyleneoxide)-block-poly(propyleneoxide)-block- poly(ethyleneoxide)-block), $EO_{20}PO_{70}EO_{20}$, molecular weight = 5800, BASF Corp.), distilled water, hydrochloric acid (HCl, 37%, Sigma Aldrich), ammonium hydroxide solution (28% in water, Fluka), aluminium nitrate ($Al(NO_3)_3$·9H2O, 98.5%, Sigma-Aldrich), magnesium nitrate ($Mg(NO_3)_2·6H_2O$, 99%, Sigma-Aldrich), nickel nitrate ($Ni(NO_3)_2·6H_2O$, 98%, Sigma-Aldrich) and cobalt nitrate ($Co(NO_3)_2·6H_2O$, 98%, Sigma-Aldrich), sodium hydroxide (NaOH), and sodium carbonate (Na_2CO_3 99.8%, Merck). For the catalytic runs, the chemicals were: styrene oxide (C_8H_8O, 98%, Sigma-Aldrich), phenylacetaldehyde (C_8H_8O, >95%%, Sigma-Aldrich), 2-phenylethanol ($C_8H_{10}O$, >99.5%, Sigma-Aldrich), 1,4-dioxane ($C_4H_8O_2$, >99.5%, Sigma-Aldrich), cyclohexanol ($C_6H_{12}O$, 99%, Sigma-Aldrich), and hydrogen (H_2, > 99.999%, Air Liquide).

Catalysts.

Al-SBA-15. Al-SBA-15 was prepared by a modified two-step ‘‘pH-adjusting’’ method as reported in Ungureanu et al.[25] Pluronic P123 is dissolved in a 2 M HCl aqueous solution. TEOS was thereafter added to the solution, and the required amount of aluminium source, to obtain a Si/Al atomic ratio of 10, was added. The resulting gel was subjected to a hydrothermal treatment at 100 °C for 48 h. At the end of the hydrothermal treatment, the pH value of the mixture was adjusted to 7.5, by using a 4 M NH_4OH solution. The mixture was again subjected to a hydrothermal treatment at 100 °C for 72 h. The final solid was separated by filtration, washed with distilled water and dried at 60 °C for 12 h. The open porous structure of Al-SBA-15 material was obtained by calcination under air at 550 °C for 6 h (heating ramp of 1.5 °C min^{-1}).

Layered double hydroxides. Me-Mg-Al ternary layered hydroxides (Me = Ni, Co), with atomic ratio Me:Mg:Al = 1:1:1, were prepared by co-precipitation under low suprasaturation method, at pH ~ 8 and T = 25 °C, using nitrates as metal sources. After aging 12 h with stirring, at 60 °C, the precipitates were filtered, washed with a carbonate solution in order to remove nitrate ions from the interlayers, and finally repeatedly washed with deionized water to remove residual sodium. The resulting precipitate was dried overnight in an oven at 40 °C. The corresponding samples are denoted as Me-LDH (Me= Ni, Co), respectively. The layered hydroxides were heated at 2 °C/min to 450 °C and kept for 6 h to obtain Me-Mg-Al mixed oxides (the samples are denoted as Me-MO(nR), where Me = Ni, Co and nR = un-reduced). Before hydrogenation reaction, the mixed oxides were reduced for 6 h in hydrogen flow at various temperatures in order to obtain supported metal samples, denoted as Me-MO(R_T), where Me is the transition metal and T is the reduction temperature.

Characterization.

Chemical composition (Mg, Co, Ni and Al) of the samples was measured on a Perkin sequential scanning inductively coupled plasma optical emission spectrometer (Optima 2000 DV). Before analysis, a known amount of sample was dissolved in a diluted HCl solution and then heated under microwave until complete dissolution.

XRD measurements were performed on a Bruker AXS D8 apparatus with monochromatic CuKα radiation (λ = 0.154184 nm) at room temperature. For Al-SBA-15, the patterns were collected in the 2θ range from 0.6 to 6 ° with a step of 0.01°. For Me-HT samples, the patterns were recorded from 5 to 70° 2θ, with a step of 0.02°. The crystallite sizes were calculated using the Scherrer equation: $d_{hkl} = \lambda/\beta\cos\theta$, where λ = incident ray wavelength (0.15406 nm); β = peak width at half height (rad) after Warren's correction for instrumental broadening; and θ = Bragg angle.

Nitrogen physisorption experiments were carried out on an Autosorb 1-MP instrument from Quantachrome at −196 °C. Surface area, pore volume and pore size distribution were obtained from the corresponding isotherms using the conventional calculation algorithms such as B.E.T., de Boer and B.J.H.

Temperature programmed reduction experiments were performed on a ChemBET PULSAR™ TPR/TPD analyzer from Quantachrome. About 30 mg of sample were inserted in a U-shape microreactor. Before each TPR run, the catalyst was activated at 120 °C for 4 h under a simulated air flow (40 mL min^{-1}). After cooling to 50 °C, the H_2 containing flow was stabilized (40 mL min^{-1}, 5 vol.% H_2 in Ar), and the TPR was performed from 50 to 900 °C with a temperature ramp of 5 °C min^{-1}.

In situ powder XRD patterns were recorded on a Bruker D8 ADVANCE X-ray diffractometer equipped with a VANTEC-1 detector, using a CuKα radiation (λ = 1.54184 Å) as X-ray source. The powder samples were placed on a kanthal filament (FeCrAl) cavity. The data were collected in the 2θ range from 10 to 80° with a step of 0.05° (step time of 2 s). Phase identification was made by comparison with ICDD database. The diffractograms were recorded after *in situ* reduction from 30 to 700 °C under a flow of 3 vol.% H_2 in He (30 mL min^{-1}). The data were collected 3 times at each temperature.

Catalytic tests.

Hydrogenation of SO and PAA. The hydrogenation catalytic runs were performed at atmospheric pressure and a constant temperature, in a two-neck glass batch reactor (50 mL), equipped with magnetic stirrer, thermometer and reflux condenser. In a typical experiment, the reactor was charged with 0.5 mL of reagent (SO or PAA), 25 mL of 1,4-dioxane (as solvent), 0.2 mL cyclohexanol (as internal standard) and 0.2 g of catalyst. Once the temperature had reached the desired value, the agitation was started (stirring rate of 900 rpm). The hydrogen was added to the reaction mixture by bubbling at a constant rate feed during the reaction test. Samples of the reaction mixture were withdrawn periodically and analyzed by GC on a Varian 3900 chromatograph (DB-1 capillary column: 60 m x 0.32 mm x 0.3 µm, FID detector). The identification of the products was achieved from the retention times of the pure compounds and by GC-MS. Quantitative analyses were performed by taking into account the FID response factors for each products.

Simultaneous reactions. The conversion of SO (0.47 mL) has been carried out with H_2 in 20 mL of 1,4-dioxane, at 90°C, by introducing 50 mg of Al-SBA-15 (Si/Al = 10) and 50 mg of Co-MO(R_{650}) at the beginning of the process.

Cascade reactions. The styrene oxide (0.47 mL) was initially isomerized into PAA in the absence of H_2, at 90 °C using 50 mg of Al-SBA-15 catalyst and 20 mL of 1,4-dioxane. After 30 min of reaction, Al-SBA-15 is filtered off the reactor, and 50 mg of Co-MO(R_{650}) was added into the reactor with the product of isomerization step. The catalytic transformation of PAA obtained from isomerisation was carried out at 90 °C, in the presence of H_2.

Results and Discussion

Characterization of materials.

Two different materials have been used as catalysts for the synthesis of 2-PEA. The first one is purely acidic and it was obtained by incorporation of aluminum into the framework of SBA-15 mesoporous silica by pH-adjusting method. Preparation of this material was fully described in our previous work.[26] Only key properties of Al-SBA-15 are provided herein to confirm the high quality of this material with respect to composition, structure and texture.

Elemental analysis for Al-SBA-15 sample confirms the total incorporation of aluminum in the final material (Table 1). Small angle XRD pattern (Figure 1A) displays three reflections indexed to the (100), (110) and (200) plans assigned to ordered two-dimensional hexagonal mesostructure of *p*6mm symmetry.

This result confirms the preservation of the SBA-15 pore structure after aluminum incorporation.

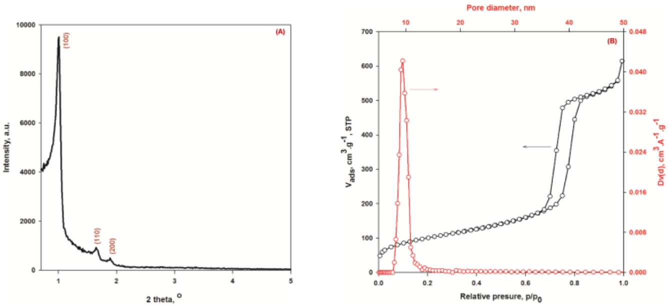

Figure 1. XRD patterns at low angles (A), and N_2 physisorption isotherm and NL-DFT pore size distribution (B) recorded for calcined Al-SBA-15 acidic catalyst.

The textural properties of Al-SBA-15 material were evaluated from data of nitrogen physisorption at -196 °C. The experimental isotherm is shown in Figure 1B, together with the pore size distribution curve. It can be observed that Al-SBA-15 solid displays an isotherm of type IV, with a H1-type hysteresis loop, which is characteristic of ordered mesoporous solids with cylindrical pore geometry. Results are in good agreement with XRD data. The pore size distribution, as evaluated by NL-DFT treatment, exhibits a narrow distribution, with an average size of 9.2 nm. Calculated textural parameters are gathered in Table 2.

The second type of material consists in non-noble metals, Ni- and Co, supported on a solid with acid-base properties *via* LDH precursors. The metallic material is prepared by calcination, followed by reduction, of a metal-containing hydrotalcite-like precursor. The as-synthesized multicomponent LDHs were characterized by ICP, XRD and N_2 physisorption, in order to assess their chemical composition, crystalline structure and textural properties. Chemical analysis confirms that the ratios between the three components constituting the LDH samples are very close to those used in the synthesis mixture, that is 1:1:1 (Table 1).

Table 2. Physico-chemical properties of samples.

Al-SBA-15			
N_2 physisorption			
Si/Al[a]			9.3
S_{BET} [b] (m^2 g^{-1})			351
V_p [c] (cm^3 g^{-1})			0.86
D_p [d] (nm)			9.2
LDH based materials			
Properties		**Ni containing materials**	**Co containing materials**
ICP (wt%)	**Ni**	34.00	-
	Co	-	35.35
	Mg	32.75	32.68
	Al	32.92	31.97
XRD-LDH[e]	***a* [e] (Å)**	3.03	3.04
	***c* [f] (Å)**	22.7	22.79
	$D_{(003)}$ [g] (nm)	3.8	9.0
	$D_{(110)}$ [h] (nm)	8.5	15.2
N_2 physisorption	**S_{BET} [b] (m^2 g^{-1})** **LDH[i]**	128	124
	MO[k]	192	191
	V_p [c] (cm^3 g^{-1}) **LDH[i]**	0.36	0.56
	MO[k]	0.47	0.67

[a] Si/Al ratio determined by ICP-OES. [b] total specific surface area obtained using the BET equation. [c] total pore volume measured at P/P_0 = 0.97. [d] average pore size evaluated by NL-DFT for cylindrical pores/equilibrium model. [e] cation–cation distance within the brucite-like layer, $a = 2d_{110}$. [f] total thickness of the brucite-like layer and the interlayer distance, $c = 3d_{003}$. [g] crystallite size in “c” direction. [h] crystallite size in “a” direction. [i] layered precursor of the catalyst. [k] Mixed Oxide.

The diffraction patterns (Figure 2) of the two as-synthesized samples show typical diffraction peaks of crystalline hydrotalcite-like material.[27]

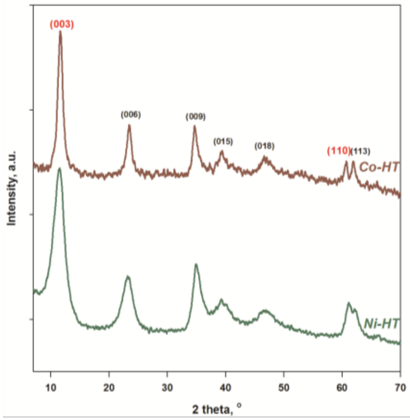

Figure 2. Powder X-ray diffraction for the as-synthesized LDHs.

As previously observed,[28] Co-LDH exhibits sharper and narrower diffraction peaks, suggesting an improved crystallinity (larger particle size, Table 2) as compared with Ni-HT. The structural parameters, *a* and *c,* as well as the crystallite sizes were calculated and included in Table 2. Obviously, the value of structural parameters changes with the material composition, since the “*a*” parameter is highly sensitive to the nature of layer cations (*i.e.*, its ionic radii).[27,29]

The nitrogen adsorption-desorption isotherms of the as-synthesized samples are of type IIb, with hysteresis loops of type H3 (not shown here), and originate from the adsorption of nitrogen in the void spaces between the plate-like particles constituting the material.[30,31] Based on these isotherms, textural properties (specific surface areas and pore volumes) have been evaluated (Table 2). Measured values are in line with those already reported for comparable materials.[27,32] The textural properties of the unreduced mixed oxides, Me-MO(nR), obtained from LDH decomposition by calcination at 450 °C, have been also evaluated. Values for surface areas and pore volumes are typical for these oxides,[33] and are higher than those displayed by the Me-LDH precursors (Table 2).

Reducibility and extent of metal–support interactions have been investigated by TPR for Me-MO(nR) materials (Figure 3).

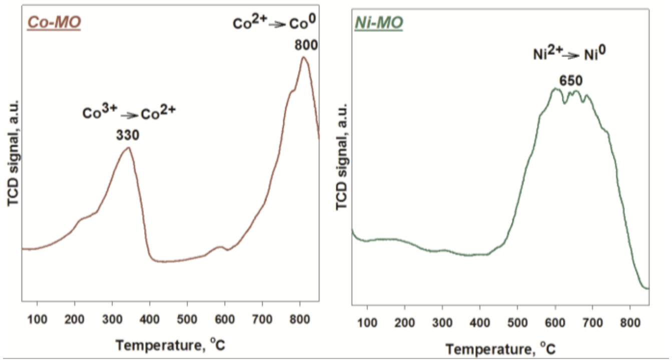

Figure 3. TPR profiles of the Me-MO(nR) samples.

The TPR profile for Co-MO(nR) displays two main reduction peaks: the first one with maximum (T_{max}) centered at ~330 °C, it is assigned to the reduction of Co_3O_4 spinel to CoO, and the second one, starting at 600 °C and centered (T_{max}) at ~800 °C, which is attributed to the reduction of CoO to Co^0. The TPR profile of Ni-MO(nR) shows only one reduction peak, between 400 and 800 °C with maximum at ~650 °C, that is assigned to the reduction of Ni^{2+} cations from NiO in strong interaction with alumina surface and/or $NiAl_2O_4$ phase.[33-36]

In order to identify the intermediate crystalline phases formed during the reduction process, Co- and Ni-MO(nR) have been reduced under hydrogen flow at different temperatures in the range of 30–700 °C and monitored *in situ* by XRD. The recorded diffractograms are displayed in Figure 4.

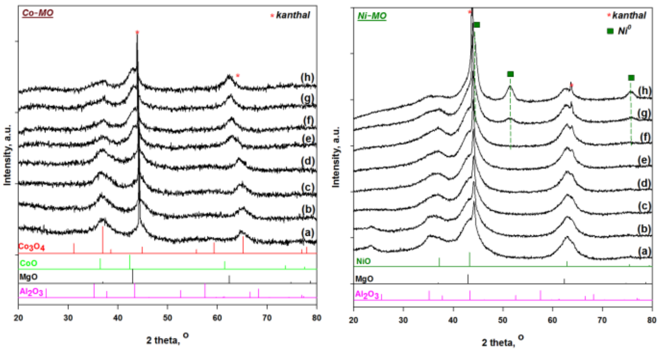

Figure 4. *In situ* reduction followed by XRD for Me-MO(nR) samples. Temperatures of reduction: (a) 30 °C, (b) 100 °C, (c) 200 °C, (d) 300 °C, (e) 400 °C, (f) 500 °C, (g) 600 °C, (h) 700 °C.

For Co-MO(nR), reflections identified in the diffractogram recorded at 30 °C fit the diffraction pattern of Co_3O_4 (ICDD 42-1467).[35,37,38] Only small peaks assigned to MgO and Al_2O_3 phases can be distinguished. This could suggest an amorphous state of these last two oxides. The diffraction peaks of Co_3O_4, detected up to 300 °C, are broad and of low intensity. This result indicates either the partial crystallization or the formation of very small Co_3O_4 nanoparticles. After reduction at 400 °C, Co_3O_4 spinel phase disappeared, while new reflections appear at 2θ = 36.47, 42.37, 61.47°. These reflections are assigned to the (111), (200) and (220) planes of the CoO crystal phase (ICDD 48-1719).[39] The intermediate CoO phase is observed to be incompletely reduced up to 700 °C, in good agreement with the TPR profile (Figure 3). However, the reflections of metallic Co^0 phase are undetectable in the diffractograms, suggesting the high dispersion of metallic species at the surface of oxide support.

For Ni-MO(nR), the diffractogram recorded at 30 °C displays reflections assigned to three different oxides, i.e., NiO, MgO and Al_2O_3. As the temperature increases, the diffraction peaks became smaller, and after reduction at 500 °C, only diffraction peaks assigned to NiO phase (ICDD 047–1049) are identified. After reduction at 600 and 700 °C, the diffraction peaks of NiO phase are still observed besides the new peaks arising at 2θ = 44.5, 51.89 and 76.45°. These last three peaks are assigned to metallic Ni^0 (ICDD 04–0850). A decrease in intensity of the NiO diffraction peaks, in parallel with a significant increase in the intensity of Ni^0 diffraction peaks, clearly indicates that NiO is mainly reduced to Ni^0 in this range of temperatures. This result is also in good agreement with TPR data that shows almost complete reduction of NiO below 700 °C (Figure 3).

Catalytic hydrogenation of SO and PAA.

In order to explore the catalytic properties of Ni- and Co-based catalysts for the selective production of 2-PEA, SO and PAA were hydrogenated in separate experiments under various reaction conditions.

Reaction pathways. The reduced Ni- and Co-catalysts convert SO into 2-PEA and EB/ST as main products of hydrogenation with H_2. 2-PEA is the expected product of the catalytic hydrogenation of SO.[13,14] ST could be produced either by SO deoxygenation (as previously reported),[13,14,22] or by 2-PEA dehydration (Scheme 1). To determine the origin of styrene, pure 2-PEA was hydrogenated at 90 °C in the presence of Ni-catalyst and 1,4-dioxane as solvent. No reaction was observed under these conditions, suggesting that SO deoxygenation is at the origin of ST formation. Ethylbenzene is reasonably formed *via* styrene oxide deoxygenation (Scheme 1).

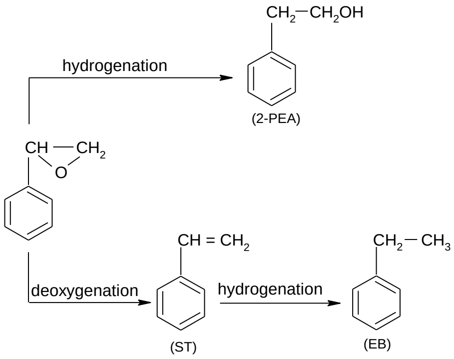

Scheme 1. Reaction pathway for SO hydrogenation

It is interesting to note that small amounts of PAA and 1-penylethanol were produced with both catalysts. The formation of such products was often reported.[11,17,22] The catalytic conversion of PAA in the presence of hydrogen gives only 2-PEA (as selective hydrogenation product), and oligomers (these mainly resulting from the aldol condensation of PAA and further transformations of dimers) (Scheme 2).

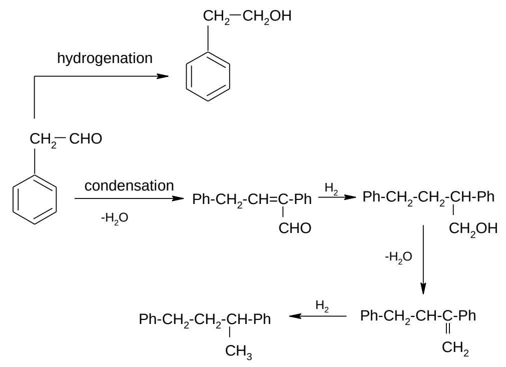

Scheme 2 Reaction pathway for PAA hydrogenation-condensation (Ph = phenyl).

Effect of the reduction temperature of the MO precursors. To obtain catalytic materials the "as-made" layered double hydroxides have been subjected to various thermal and/or chemicals treatments. The samples were then used as catalysts in the hydrogenation of SO.

Mixed oxides, Me-MO(nR), obtained from Me-LDH by calcination at 450 °C, without reduction. No reaction occurs with SO when the hydrogenation is carried out at 90 °C in 1,4-dioxane as solvent. By contrary, significant condensation of PAA is observed.

Reduced mixed oxides, Me-MO(R_T), obtained from Me-MO(nR), by reduction under hydrogen (T = applied reduction temperature). Materials obtained by reduction at various temperatures from 400 to 700 °C have been used for the hydrogenation of SO at 90 °C. As shown in Figure 5, the reduction temperature has a significant effect on the SO conversion. With Ni-MO(R_T), a volcano-shaped dependence of the activity, with a maximum after reduction at 500 - 550 °C, was obtained. This temperature is in good agreement with the TPR data, which indicated that above 500 °C, nickel species are reduced to Ni^0. In the case of Co-MO(R_T), samples reduced at temperatures lower than 550 °C are inactive. The SO conversion remains at low level for Co-MO(R_{550}) and Co-MO(R_{600}), and it reaches a maximum for Co-MO(R_{650}) and then slightly decreases at higher temperature. This result is in agreement with TPR data showing that the reduction of CoO into Co^0 is effective above 600 °C (Figure 3).

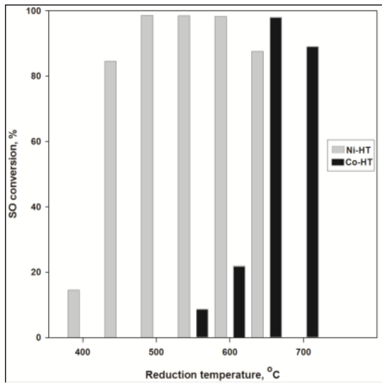

Figure 5. Effect of the reduction temperature of Me-MO(R_T) on SO conversion (Reaction conditions: T = 90 °C, time = 120 min).

Non-calcined Me-LDH, reduced with hydrogen at 500 °C (Me = Ni) and at 650 °C (Me = Co). The two catalysts showed similar behavior for the hydrogenation of SO, in terms of activity and selectivity, as the calcined and reduced counterparts.

Kinetic profile of SO and PAA hydrogenation. Figure 6A and B show the kinetic profiles of the conversion of SO and PAA as a function of reaction time at 90 °C, over Ni-MO(R_{500}) and Co-MO(R_{650}) catalysts. The results show that for both organic reagents, Ni-based catalyst is more active than Co-based catalyst, but, it is worth to mention, significant conversions of SO and PAA can be reached on both catalysts after 300 min of reaction.

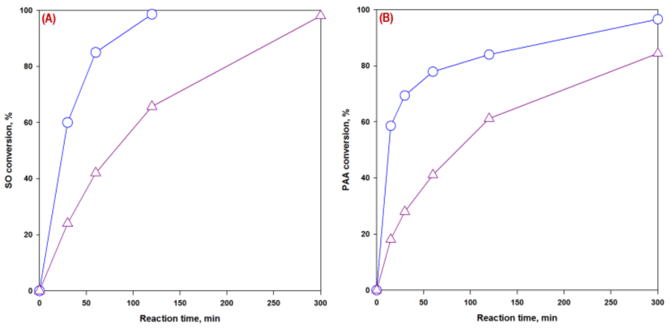

Figure 6. Kinetic profile of SO (A) and PAA (B) hydrogenation reaction at 90°C over Ni-MO(R_{500}) (o), and Co-MO(R_{650}) (Δ).

Selectivity in hydrogenation. Tables 3 and 4 summarize the reagent conversions and product distributions obtained in the hydrogenation of SO and PAA catalysed by materials obtained by reduction at different temperatures, and under various reaction conditions. With Ni-MO(R_T), the main hydrogenation products of SO at 90 °C are 2-PEA and EB. The 2-PEA to EB ratio is strongly influenced by the hydrogenation temperature, but only slightly by the reduction temperature of the catalyst (Table 3). Indeed, under similar conditions, the selectivity to 2-PEA significantly increased when the hydrogenation temperature decreased from 90 to 60 and 40 °C. Note that during the first minutes of reaction, the formation of 1-2% of ST was observed, which was thereafter hydrogenated into EB (Scheme 1).

Table 3. Conversions and product distributions in SO hydrogenation.

Catalyst	T_{red}[a], °C	T_r,[b] °C	t_r,[c] min	SO conversion, %	Products, mol%		
					2-PEA	ST	EB
Ni-MO[d]	400	90	360	40.8	75.8	-	24.2
	450	90	180	96.9	72.6	-	27.4
	500	90	120	98.6	73.0	-	27.0
	500[e]	90	120	96.2	69.9	-	30.1
	500	60	300	98.3	88.9	-	11.1
	500	40	360	84.7	95.0	-	5.0
	550	90	120	98.5	71.5	-	28.5
	600	90	120	98.3	68.5	-	31.5
	650	90	180	87.6	69.4	-	30.6
Co-MO[d]	500	90	360	8.6	23.0	76.9	0.1
	600	90	480	21.9	32.2	67.6	0.2
	650	60	360	37.6	33.2	65.6	1.2
	650	90	300	98.0	41.2	58.6	0.2
	700	90	300	89.0	38.8	61.0	0.2
	650[e]	90	300	96.5	38.0	61.9	0.1

[a] reduction temperature. [b] reaction temperature. [c] reaction time. [d] samples obtained from (Ni)Co-LDH by calcination at 450 °C and reduction with H_2. [e] sample obtained by reducing of "as made" LDH.

In the presence of Co-MO(R_T), the main hydrogenation product was ST (> 60%), and its amount depends on the reduction temperature and SO conversion (Table 3). As a general trend, the ST to 2-PEA ratio decreased as the SO conversion increased. Only traces of EB are detected regardless of the hydrogenation and reduction temperatures. It is important to note that the direct deoxygenation of epoxides into the corresponding alkenes is an useful reaction because it allows the use of oxirane rings as protecting groups for C=C double bonds. Traditionally, this reaction has been conducted using stoichiometric amounts of reagents or in the presence of PPh_3, Na/Hg or $NaBH_4$ as reducing agents. Recently, Noujima *et al.*[40] demonstrated that gold nanoparticles supported on hydrotalcite is an efficient heterogeneous catalyst for the deoxygenation of epoxides to alkenes with H_2. The hydrotalcite as support seemed to play a crucial role for this behavior. Our results suggest that Co-MO(R_T) materials could be also considered as interesting catalysts for the deoxygenation of epoxides into alkenes. In addition, cobalt based catalysts have the advantage of being cost effective and easily available in comparison to noble metals.

Table 4. Conversions and product distributions in PAA hydrogenation.

Catalyst	T_{red}[a], °C	T_r,[b] °C	t_r,[c] min	PAA conversion, %	Products, mol%	
					2-PEA	Oligo[d]
Ni based catalysts						
MO[e]	-	90	150	35	-	100
Ni-MO[f]	500	90	15	59	17	83
	500	90	300	96.6	23.3	76.7
	650	90	360	92.2	72.8	27.2
	500	60	150	55.9	93.1	6.9
Co based catalysts						
MO[e]	-	90	180	68.6	-	100
Co-MO[f]	650	90	15	18	85.3	14.7
	650	90	300	84.4	96.5	3.5

[a] reduction temperature. [b] reaction temperature. [c] reaction time. [d] oligomers, according to Scheme 2. [e] samples obtained from (Ni)Co -LDH by calcination at 450 °C and reduction with H_2. [f] samples obtained from (Ni)Co-MO by reduction with H_2.

In the hydrogenation process of PAA, performed in the presence of Me-MO(nR), no hydrogenation products are formed, but significant amounts of oligomers (as condensation products) are produced (Table 4 and Scheme 2). With Ni-MO(R_T) and Co-MO(R_T), both 2-PEA and oligomers were produced. For Ni-MO(R_T), the reduction temperature and the reaction temperature have both crucial effects on the 2-PEA selectivity. Indeed, at 90 °C, selectivities of 23.3% and 72.8% are obtained for Ni-MO(R_{500}) and Ni-MO(R_{650}), respectively. However, in the case of Ni-MO(R_{500}) catalyst, the decrease of reaction temperature at 60 °C allows to increase the 2-PEA selectivity. Also, the amount of 2-PEA increased when the PAA conversion increases, irrespective of the reaction temperature. In the case of Co-MO(R_{650}), 2-PEA was the main product in the PAA hydrogenation (Table 4); its selectivity reaches 96.5% when the conversion reaches 84.4%.

Table 4 also shows that the PAA condensation into oligomers may be catalyzed either by Me-MO(nR) (consisting in a mixture of (Ni)Co, Mg and Al oxides) or by Me-MO(R_T) (metallic (Ni)Co besides Mg and Al oxides). Accordingly, it is reasonable to consider that the catalytic sites for the aldehyde condensation are located on the MgO and/or Al_2O_3 surface. Indeed, remarkable activities of MgO and mixed oxides (obtained from Mg/Al-LDH decomposition) for the aldol condensation reactions was already reported.[41-43] Only Co-MO(R_{650}) does not significantly catalysed the PAA condensation reaction. After reduction at 650 °C, the material contains only small amount of isolated oxide species like MgO and Al_2O_3, that can explain this result. An additional proof is the behaviour of Ni-MO(R_{650}) for which the PAA conversion into oligomers is substantially reduced as compared with the results obtained with the sample reduced at lower temperature (Table 4). The modification/disappearance of the MgO and Al_2O_3 phases during the treatment at high temperature was clearly showed above (Figure 4).

Leaching test. In order to demonstrate the real heterogeneous character of the reaction, and that the catalytic activity does not originate from cationic cobalt dissolved from the heterogeneous catalyst, additional catalytic test was performed with PAA as reagent. The catalyst was filtered off at 90 °C after 120 min reaction (60 % conversion) then the solution was further allowed to react for 120 min at 90 °C. Conversion of PAA remains constant, indicating that the catalytic process is purely heterogeneous.

Catalytic cascade reactions.The results presented above indicate that significant amounts of ST or EB are formed during the SO hydrogenation over Co- and Ni-MO(R_T), depending on the nature of metallic active phases. Similarly, the hydrogenation of PAA into 2-PEA is accompanied by the formation of large amounts of by-products like oligomers over Ni-MO(R_T) catalyst. Instead, the hydrogenation of PAA is highly selective to 2-PEA when Co-MO(R_T) is used as catalyst. This behaviour can be rationalized in term of d-band width of the metals. Accordingly, those metals having narrower d-band width are better catalysts for hydrogenation of C=C bond (e.g., Ni - 3.0 eV) while for those with larger width, the interaction of the metal surface with the C=O bond is greater than with the olefin bond (e.g., Co – 4.0 eV). [44,45] On the other hand, we have shown in a previous study that SO can be easily and selectively isomerised into PAA over Al-SBA-15 (predominantly weak-moderate acid catalyst), under mild reaction conditions, which limits the occurrence of secondary reactions with the highly reactive PAA (i.e., oligomerization).[26]

Combining these results with the present ones, a two-step process including the SO isomerization into PAA (over Al-SBA-15 catalyst), and the PAA hydrogenation into 2-PEA (over Co-MO(R_T) catalyst) has been considered. In this regard, two routes were approached: (i) one-pot process, when Al-SBA-15 and Co-MO(R_{650}) were simultaneously added ab initio; (ii) sequential process, when SO isomerization into PAA is firstly carried out over Al-SBA-15, then it is followed by PAA hydrogenation over Co-MO(R_{650}) in separate runs.

Using the first approach, the conversion of SO was complete after 30 min of reaction and that of PAA was 93% after 120 min. The products consisted of 80.7% of 2-PEA, 13% of styrene, 1.6% of EB and 4.7% oligomers. These results show that the approach does not allow to produce selectively 2-PEA from SO.

When the two catalysts were consecutively added into reaction solution, the conversion of PAA was 76% and 90% after 180 and 300 min, respectively. The final product consisted of 98% of 2-PEA and only 2% of oligomers. No styrene and EB formation is observed. This approach ensure a selective production of 2-PEA from SO. This result is as good as the representative performances previously reported for the direct hydrogenation of SO to 2-PEA, with different catalysts, under various conditions (Table 1). It is important to note that the best previous results were obtained either over noble metals (sometimes in an alkaline medium) or with Ni-based catalysts at a high catalyst/SO ratio.

As it is known, SO can also be easily prepared by epoxidation of ST over titanium containing microporous and mesoporous materials.[46] A feasible process to obtain 2-PEA with high selectivity from styrene can be also proposed. The integrated system includes 3 consecutive selective reactions, catalyzed by three different materials, as follows: (i) the conversion of styrene to SO by clean oxidation with H_2O_2 catalyzed by a microporous titanosilicalite, TS-1,[46] followed by (ii) the isomerization of SO into PAA over Al-SBA-15, and finally, (iii) the hydrogenation of PAA to 2-PEA over Co-MO(R_T) (Scheme 3).

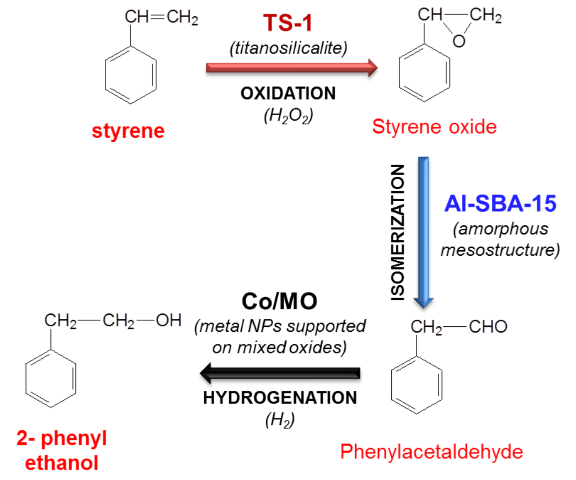

Scheme 3. Three-step cascade reactions for the selective preparation of 2-PEA, starting from ST precursor.

The proposed approach, in three cascade reaction, is a very promising way to selectively transform ST to 2-PEA using green efficient process involving the use of heterogeneous catalysts.

Conclusions

Selective production of 2-PEA were investigated by using Co- and Ni-based catalysts, supported on $MgO-Al_2O_3$ homogeneous mixed oxides. Active catalysts were obtained by calcination of corresponding LDH precursors, and then reduced under H_2. SO and PAA were both used as starting molecules for the synthesis of 2-PEA.

When SO was used as starting molecule and metallic nickel as active phase, low reaction temperatures were favorable to the hydrogenation of SO to 2-PEA. Using metallic cobalt as active phase, deoxygenation of SO to ST occurred.

When PAA was used as starting molecule, the selectivity to 2-PEA was controlled by both reduction and reaction temperatures, over metallic nickel containing material. Instead, when metallic cobalt containing catalyst was used under comparable reaction conditions, this is significantly more selective to 2-PEA than Ni-based catalyst.

On the basis of these results, a new and efficient strategy to produce selective 2-PEA from SO was proposed on the basis of catalytic cascade reactions (*i.e.*, isomerization of SO over acidic Al-SBA-15 catalyst, followed by hydrogenation over metallic cobalt containing active material). From this approach, an extend strategy of selective synthesis of 2-PEA by three-step catalytic process could be suggested, including also the epoxidation of ST to SO over titanium containing zeolites.

Acknowledgements

This work was partially supported by a grant of the Romanian National Authority for scientific Research, CNCS – UEFISCDI, project number PN-II-RU-TE-2012-3-0403.

References

1 C.Jr. Huang, S.L. Lee and C.C. Chou, *J Biosci Bioeng*, 2000, **90**, 142;
2 M.M.W. Etschmann, W. Bluemke, D. Sell and J. Schrader, *Appl Microbiol Biotechnol*, 2002, **59**, 1;
3 D. Hua and P. Xu, *Biotechnol Adv*, 2011, **29**, 654.
4 A. Karami, A. Niazi, G. Kavoosi, M. Khosh-Khui and H. Salehi, *Physiol Mol Biol Plants,* 2015, **21**, 43.
5 R.V. Chaudhari, M.M. Telka and C.V. Zaccheria, 2000, US Patent 6166269.
6 C. Shell, *Ingredients for the Modern Perfumery Industry, in: The Chemistry of Fragrances*, (Eds.: D. Pybus, C. Shell), RSC Publishing, Cambridge, UK, 2006, pp. 101-102.
7 S.C. Laha and R. Kumar, *J Catal,* 2001, **204**, 64.
8 J. Song, Z. Zhang, T. Jiang, S. Hu, W. Li, Y. Xie and B. Han, *J Mol Catal A: Chem,* 2008, **279**, 235.
9 S. Mitsui, S. Imaizumi, M. Hisashige and Y. Sugi, *Tetrahedron*, 1973, **29**, 4093.
10 V.G. Yadav and S.B. Chandalia, *Org Proc Res Develop*, 1998, **2**, 294.
11 I. Vicente, P. Salagre and Y. Cesteros, *Appl Clay Sci*, 2011, **53**, 212.
12 I. Vicente, P. Salagre and Y. Cesteros, *Appl Catal A : Gen*, 2011, **408**, 31.
13 C.V. Rode, M.M. Telkar and R.V. Chaudhari, *Stud Surf Sci Catal*, 2000, **130**, 533.
14 O. Bergada, P. Salagre, Y. Cesteros, F. Medina and J.E. Sueiras, *Appl Catal A-Gen*, 2007, **331**, 19.
15 O. Bergada, P. Salagre, Y. Cesteros, F. Medina and J.E. Sueiras, *Catal Lett*, 2008, **122**, 259.
16 O. Bergada, P. Salagre, Y. Cesteros, F. Medina and J.E. Sueiras, *Appl Catal A-Gen*, 2004, **227**, 125.
17 I. Kirm, F. Medina, X. Rodriguez, Y. Cesteros, P. Salagre and J.E. Sueiras, *J Mol Catal A: Chem*, 2005, **239**, 215.
18 C.V. Rode, M.M. Telkar, R. Jaganathan and R.V. Chaudhari, *J Mol Catal A: Chem*, 2003, **200**, 279.
19 A.A. Dabbawala, N. Sudheesh and H.C. Bajaj, *Dalton Trans*, 2012, **41**, 2910.
20 G.D. Yadav and Y.S. Lawate, *J Supercrit Fluids*, 2011, **59**, 78.
21 G.D. Yadav and Y.S. Lawate, *Ind Eng Chem Res*, 2013, **52**, 4027.
22 I. Kirm, F. Medina, J.E. Sueiras, P. Salagre and Y. Cesteros, *J. Mol Catal A: Chem*, 2007, **261**, 98.
23 M.M. Telkar, C.V. Rode, R.V. Chaudhari, S.S. Joshi, and A.M. Nalawade, *Appl Catal A-Gen*, 2004, **273**, 11.

24 H. Fujitsu, S. Shirahama, E. Matsumura, K. Takeshita and I. Mochida, *J Org Chem*, 1981, **46**, 2287.
25 D. Poondi and M.A. Vannice, *J Mol Catal A: Chem*, 1997, **124**, 79.
26 A. Ungureanu, B. Dragoi, V. Hulea, T. Cacciaguerra, D. Meloni, V. Solinas and E. Dumitriu, *Microporous Mesoporous Mater*. 2012, **163**, 51.
27 F. Cavani, F. Trifirò and A. Vaccari, *Catal Today*, 1991, **11**, 173.
28 C. Rudolf, B. Dragoi, A. Ungureanu, A. Chirieac, S. Royer, A. Nastro and E. Dumitriu, *Catal Sci Technol*, 2014, **4**, 179.
29 V. Rives, *Mater Chem Phys*, 2002, **75**, 19.
30 P. Benito, F. M. Labajos, J. Rocha and V. Rives, *Microporous Mesoporous Mater*, 2006, **94**, 148.
31 V. Rives, in: *Layered Double Hydroxides: Present and Future*, ed. V. Rives, Nova Science Publishers, New York, 2001, pp. 243.
32 J. M. Fernandez, C. Barriga, M. A. Ulibarri, F. M. Labajos and V. Rives, *Chem Mater*, 1997, **9**, 312.
33 S. Ribet, D. Tichit, B. Coq, B. Ducourant and F. Morato, *J Solid State Chem*. 1999, **142**, 382.
34 F. Bentaleb and E. Marceau, *Microporous Mesoporous Mater*, 2012, **156**, 40.
35 S. Velu, K. Suzuki, M. P. Kapoor, S. Tomura, F. Ohashi and T. Osaki, *Chem Mater*, 2000, **12**, 719.
36 V. Rives, M. A. Ulibarri, A. Montero, *Appl Clay Sci*, 1995, **10**, 83.
37 X. Ke, J. Cao, M. Zheng, Y. Chen, J. Liu and G. Ji, *Mater Lett*, 2007, **61**, 3901.
38 M. A. Ulibarri, J. M. Fernandez, F. M. Labajos and V. Rives, *Chem Mater*, 1991, **3**, 626.
39 Z. Wen, F. Zheng, Z. Jiang, M. Li and Y. Luo, *J Mater Sci*, 2013, **48**, 342.
40 A. Noujima, T. Mitsudome, T. Mizugaki, K. Jitsukawa and K. Kaneda, *Angew Chem Int Ed*, 2011, **50**, 2986.
41 E. Dumitriu, V. Hulea, N. Balba, G. Carja and A. Azzouz, *J Mol Catal A: Chem*, 1993, **79**, 175.
42 E. Dumitriu, V. Hulea, C. Chelaru, C. Catrinescu, D. Tichit and R. Durand, *Appl Catal A-Gen*, 1999, **178**, 145.
43 D. Tichit, D. Lutic, B. Coq, R. Durand and R. Teissier, *J Catal*, 2003, **219**, 167.
44 F. Delbeq and P. Sautet, *J Catal*, 1995, **152**, 217.
45 U.K. Singh and A.M. Vannice, *J Catal*, 2001, **199**, 73.
46 V. Hulea and E. Dumitriu, *Appl Catal A-Gen*, 2004, **277**, 99.

Table of contents entry

GA:

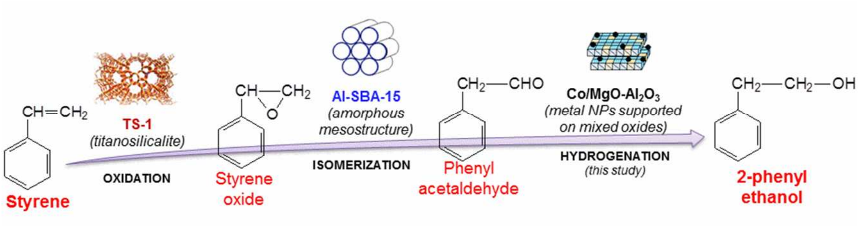

Text:

Three cascade reactions using green efficient processes involving heterogeneous catalysts are proposed to selectively obtain 2-phenyl ethanol from styrene.